Fermilab PUB-18-488-AE

MNRAS **000**, 1–11 (2018) Preprint 14 September 2018 Compiled using MNRAS LaTeX style file v3.0

Dark Energy Survey Year 1 Results: The effect of intra-cluster light on photometric redshifts for weak gravitational lensing

D. Gruen,[1,2]⋆ Y. Zhang,[3] A. Palmese,[4,3] B. Yanny,[3] V. Busti,[5,6] B. Hoyle,[7,8] P. Melchior,[9] C. J. Miller,[10,11] E. Rozo,[12] E. S. Rykoff,[1,2] T. N. Varga,[7,8] F. B. Abdalla,[4,13] S. Allam,[3] J. Annis,[3] S. Avila,[14] D. Brooks,[4] D. L. Burke,[1,2] A. Carnero Rosell,[6,15] M. Carrasco Kind,[16,17] J. Carretero,[18] R. Cawthon,[19] M. Crocce,[20,21] C. E. Cunha,[1] L. N. da Costa,[6,15] C. Davis,[1] J. De Vicente,[22] S. Desai,[23] H. T. Diehl,[3] J. P. Dietrich,[24,25] A. Drlica-Wagner,[3] B. Flaugher,[3] P. Fosalba,[20,21] J. Frieman,[3,19] J. García-Bellido,[26] E. Gaztanaga,[20,21] D. W. Gerdes,[10,11] R. A. Gruendl,[16,17] J. Gschwend,[6,15] D. L. Hollowood,[27] K. Honscheid,[28,29] D. J. James,[30] T. Jeltema,[27] E. Krause,[31] R. Kron,[3,19] K. Kuehn,[32] N. Kuropatkin,[3] O. Lahav,[4] M. Lima,[5,6] H. Lin,[3] M. A. G. Maia,[6,15] J. L. Marshall,[33] F. Menanteau,[16,17] R. Miquel,[34,18] R. L. C. Ogando,[6,15] A. A. Plazas,[35] A. K. Romer,[36] V. Scarpine,[3] I. Sevilla-Noarbe,[22] M. Smith,[37] M. Soares-Santos,[38] F. Sobreira,[39,6] E. Suchyta,[40] M. E. C. Swanson,[17] G. Tarle,[11] D. Thomas,[14] V. Vikram,[41] and A. R. Walker[42]

(DES Collaboration)

Affiliations are listed at the end of the paper.

14 September 2018

ABSTRACT

We study the effect of diffuse intra-cluster light on the critical surface mass density estimated from photometric redshifts of lensing source galaxies, and the resulting bias in a weak lensing measurement of galaxy cluster mass. Under conservative assumptions, we find the bias to be negligible for imaging surveys like the Dark Energy Survey (DES) with a recommended scale cut of ≥ 200kpc distance from cluster centers. For significantly deeper source catalogs from present and future surveys like the Large Synoptic Survey Telescope (LSST) program, more conservative scale and source magnitude cuts or a correction of the effect may be necessary to achieve per-cent level lensing measurement accuracy, especially at the massive end of the cluster population.

Key words: cosmology: observations – galaxies: distances and redshifts – galaxies: clusters: general – gravitational lensing: weak

---

⋆ E-mail: dgruen@stanford.edu; Einstein Fellow

1 INTRODUCTION

Weak lensing mass calibration is a key to achieving the full potential of galaxy cluster cosmology (for a discussion, see e.g. von der Linden et al. 2014). Numerous lensing studies have provided cluster mass estimates over the last years (e.g. Gruen et al. 2014; von der Linden et al. 2014; Hoekstra et al. 2015; Okabe & Smith 2016; Simet et al. 2017; Melchior et al. 2017; Dietrich et al. 2017a; McClintock et al. 2018). The statistical power of such analyses is continuously growing with precise gravitational shear catalogs around large cluster samples coming from DES,[1], HSC,[2] and KiDS[3], and future Euclid,[4] LSST,[5] or WFIRST[6] data. This improvement in statistics requires an equivalent push for reducing systematic uncertainties in measurement and modeling of lensing signals. State-of-the-art studies account for systematic effects such as deviations of the assumed model of the cluster matter density profile from the truth (e.g. Becker & Kravtsov 2011), systematics in background galaxy shape catalogs (e.g. Zuntz et al. 2017), excess contamination of the background source catalog with cluster member galaxies (e.g. Melchior et al. 2017; Medezinski et al. 2017), and biases and calibration uncertainties in source photometric redshifts inherent to the algorithms used for estimating them (e.g. Gruen & Brimioulle 2016; Hoyle et al. 2017). In recent studies, each of these effects cause uncertainty on cluster mass at the level of one to a few per cent (e.g. Melchior et al. 2017).

In this paper, we investigate another effect on redshift estimates of weak lensing sources – the bias due to contamination of source photometry from diffuse intra-cluster light (ICL). In our ICL model, we consider light from the central galaxy and from unbound stars in the cluster potential (see examples of studies or reviews in Zwicky 1951, 1952; Gonzalez et al. 2005; Zibetti et al. 2005; Mihos 2015; Montes & Trujillo 2018; Kravtsov et al. 2018) as well as the light of faint member galaxies below the survey selection threshold. The diffuse light biases the flux and color measurements of field galaxies, and causes a systematic change in photometric estimates of their redshift distributions. Among other effects, the spectral energy distribution (SED) of passive stellar populations at the cluster redshift introduces a mild cluster rest-frame D4000 break to the observed SED of the background galaxy. These changes in flux and color affect the redshift assigned, especially for star-forming galaxies with weaker break features.

Careful analysis of color-magnitude space could be used to select galaxies less susceptible to these effects, and composite models for blended galaxies could in principle fully account for them. Given the complexity and algorithm dependence of source photometry and redshift estimation, we do not aim to provide a prescription for correcting ICL photo-z contamination in this paper. Our goal is rather to evaluate approximately and, if possible, conservatively, what amplitude of bias we expect and identify the regimes in which it can be ignored.

In section 2, we derive our estimate for how diffuse intra-cluster light of given surface brightness biases the lensing amplitude predicted from source photometric redshifts, based on Gruen & Brimioulle (2016). In section 3, we describe our model for the surface brightness of intra-cluster light, using the results of Zhang (2018). Section 4 combines these two components of the model to estimate the bias in lensing excess density profiles in a typical current (DES-like) and future (LSST-like) survey, as a function of cluster redshift and separation from the cluster center. We conclude the study in section 5.

Estimates of a quantity q are denoted as $\hat{q}$. All magnitudes given in the $u^{\star}g'r'i'z'$ bands are in CFHT/Megacam filters[7] u.MP9301, g.MP9401, r.MP9601, i.MP9701, z.MP9801 and AB units until otherwise noted. Surface brightnesses are given in nJy arcsec^{-2} units, which can be converted to counts per arcsec^2 at a magnitude zeropoint of 30 with a conversion factor of 3.631 nJy per count. Cosmological distances for the scaling of lensing signal amplitudes are calculated in a flat Λ cold dark matter cosmology with $\Omega_{m,0} = 0.27$, and masses are expressed assuming a Hubble constant $H_0 = 70$km s^{-1} Mpc^{-1}.

2 LENSING PHOTO-Z BIASES FROM DIFFUSE LIGHT

The goal of this section is to derive a model for the bias in the lensing measurement of cluster surface matter density due to leakage of ICL into lensing source galaxy photometry used for photo-z. The source redshift dependent quantity needed for lensing measurements of a matter distribution at redshift z_d is the predicted amplitude of the lensing signal. This amplitude is proportional to

$$\beta = D_{ds}/D_s \, , \tag{1}$$

the ratio of angular diameter distances between lens and source and to the source. The true value of β could be calculated if redshifts were known for sources and lenses. In practice, the source redshift distributions are estimated from their photometry. Any bias in photo-z thus manifests as a bias in the amplitude $\hat{\beta}$ estimated from them. In this work, we therefore primarily consider biases in $\hat{\beta}$, rather than in the redshift distribution more generally.

We define this bias as

$$\left(\hat{\beta}/\beta\right) - 1 \approx F(f_{\rm ICL}, z_d, \text{source depth}) \, , \tag{2}$$

where $f_{\rm ICL}$ is the surface brightness of intra-cluster light present at the position of the background galaxy in question and z_d is the redshift of the lens. F is the model for the ICL-related bias we derive in this section. The larger the statistical power of a lensing survey, the smaller a bias can be tolerated before it significantly affects the analysis. Current (and future) surveys aim for multiplicative biases to be below the few (to one) per cent level.

In the remainder of this section we describe the basic lensing formalism, followed by our framework for estimating

---

[1] https://www.darkenergysurvey.org
[2] http://hsc.mtk.nao.ac.jp/ssp/
[3] http://kids.strw.leidenuniv.nl/
[4] https://www.euclid-ec.org/
[5] https://www.lsst.org/
[6] https://wfirst.gsfc.nasa.gov/
[7] http://cfht.hawaii.edu/Instruments/Filters/megaprime.html

the impact of ICL on empirical redshift estimates in subsection 2.1. We then develop the right hand side of Equation 2 in subsection 2.2. In this, $f_{\rm ICL}$ is denoting the level of ICL surface brightness at the position of the background galaxy population – the model for $f_{\rm ICL}$ as a function of cluster mass, redshift, and distance from the cluster center is not required for this derivation and presented later in section 3.

The image of a background source (or ensemble of sources) located on some annulus around a gravitational lens is subject to tangential gravitational shear (e.g. Bartelmann & Schneider 2001, for a review)

$$\gamma_t = \Sigma_{\rm crit}^{-1} \times \Delta\Sigma = \frac{4\pi G D_d}{c^2}\frac{D_{ds}}{D_s} \times \Delta\Sigma \equiv \frac{4\pi G D_d}{c^2} \times \beta \times \Delta\Sigma\ . \tag{3}$$

D_d, D_s, D_{ds} are the angular diameter distances to the lens, source, and between lens and source, respectively, defined as the ratios of physical to angular sizes. The excess surface density $\Delta\Sigma$ at radius r is the difference of the mean mass per area *inside* and *on the edge* of a circle of radius r,

$$\Delta\Sigma(r) = \langle\Sigma(<r)\rangle - \Sigma(r)\ . \tag{4}$$

$\hat{\beta}$ can be estimated from the photo-z redshift probability density $\hat{p}(z)$ as

$$\hat{\beta} = \int \hat{p}(z)\frac{D_{ds}(z_d, z)}{D_s(z)}\,\mathrm{d}z\ . \tag{5}$$

For the mean shear signal of an ensemble of source galaxies i, each with weight w_i, this can be written as

$$\hat{\beta} = \frac{\sum_i w_i \times \hat{\beta}_i}{\sum_i w_i}\ , \tag{6}$$

where w_i is a source weight and $\hat{\beta}_i$ the estimated β of source i from Equation 5. For the optimal (minimum variance) estimator of mean shear or surface mass overdensity, $w_i \propto \beta_i/\sigma^2_{e,i}$, or, in practice, $\propto \hat{\beta}_i/\sigma^2_{e,i}$ where σ^2_e is the shape noise variance including intrinsic and measurement noise.

In the case of an unbiased estimate $\hat{\beta}$, this connects mean tangential shear $\langle\gamma_t\rangle$ and excess surface mass density $\Delta\Sigma$ as

$$\langle\gamma_t\rangle = \frac{\sum_i w_i \times \gamma_{t,i}}{\sum_i w_i} = \frac{4\pi G D_d}{c^2} \times \hat{\beta} \times \Delta\Sigma \tag{7}$$

Thus, for example, if $\hat{\beta}$ is biased low, e.g. due to a bias in photo-z, the estimated $\Delta\Sigma$ is biased high, and vice versa.

2.1 Framework for empirical redshift estimation

Our framework for estimating the effect of ICL on photo-z is a simple empirical method that gives an unbiased estimate of $p(z|\boldsymbol{m})$, where $\boldsymbol{m}$ is a vector of colors and magnitude. Given this, and a model for the color of and total flux from diffuse light that enters each source, we can estimate how much the $\hat{\beta}$ of Equation 6 will be biased. We use this simple empirical method as a proxy for any photometric redshift estimation that could be performed using similar wide-band survey data, e.g. from DES or, with the caveat that the larger depth is not fully covered by our CFHT-based reference catalogs, LSST.

The empirical method is a simple decision tree described in detail in Gruen & Brimioulle (2016) and publicly available at https://github.com/danielgruen/betatree/. Given a complete reference sample of galaxies with photometric measurements in a set of bands and with known true redshift, the decision tree provides an unbiased and close to optimal estimate of $p(z)$ based on the color-magnitude information in any subset of these bands. The method splits the color-magnitude space spanned by the subset of bands into hyper-rectangles (boxes), and assigns to each galaxy as its $p(z)$ the histogram of true redshifts of reference galaxies in that box. We make the simplifying assumption that the lensing source sample is a magnitude limited sample of galaxies. For the purpose of these tests, and because no complete, magnitude limited sample of galaxies with spectroscopic z at sufficient depth is available, we use the same photo-z sample and (unless otherwise noted) the same settings of the tree as in Gruen & Brimioulle (2016). The galaxies used are measured from the Canada-France-Hawaii Telescope Legacy Survey (CFHTLS) Deep fields, four fields with one sq. deg. area each, for which 8-band photometry from CFHTLS and the WIRCam Deep Survey (WIRDS) is available. The sample is complete to $i' \approx 25$, although we use a shallower magnitude limited sample for all analyses to follow.

Operationally, we estimate the bias of photo-z due to intra-cluster light with the following procedures.

(i) Build a decision tree from magnitude limited sample $20 \leq i' \leq 24$ (23.5, 24.5 as variants), optimized for a cluster redshift z_d, from $g'r'i'z'$ (also $u^\star g'r'i'z'$ as a variant) color-magnitude information.

(ii) Estimate $\hat{\beta}$ in each leaf of the decision tree as the mean of β_i of all reference galaxies in that leaf.

(iii) Determine the ICL $X - i'$ color c_X as the median of the $X - i'$ color of all galaxies in the reference catalogs with $z \in [z_d - 0.02, z_d + 0.02]$ and a best-fit spectral energy distribution (SED) of a passive galaxy, where X is one of $(u^\star)g'r'z'$. Note that this assumes that the ICL has the same SED as a red galaxy: this condition is satisfied in the clusters studied in Zhang (2018), where the ICL colors are consistent with those from redMaPPer (Rykoff et al. 2014) centrals within the inner 10 kpc, becoming bluer in the outer regions but still consistent with the red sequence galaxy population. Likewise, DeMaio et al. (2018) found that ICL colors are consistent with red sequence galaxies over a wider redshift range ($0.29 < z < 0.89$) using HST imaging.

(iv) generate ICL-contaminated fluxes of each reference galaxy as $f_X^{\rm cont.} = f_X + \mu_A \times A \times f_{ICL,i} \times 10^{-0.4 c_X}$. In this, A is defined to be the area of a circle with the post-seeing half-light radius of the galaxy. In our tests, we homogenized the data to a seeing half-light radius of 0.4” to make this independent of the observing conditions of the CFHTLS-Deep fields. The factor μ_A accounts for the effective sensitivity of a method of measuring galaxy fluxes to diffuse light. We note that μ_A will depend strongly on the method used for extracting fluxes. By running SExtractor in dual-image mode with a detection image contaminated with diffuse flux, we find $\mu_A = 2.5$ for `DETMODEL` model-fitting fluxes, which are likely most similar to the model-fitting fluxes used by DES. This is thus the value we use in the following analysis. We find that the local background subtraction implicit to SExtractor `AUTO` photometry makes extracted fluxes insensitive to a diffuse background, i.e. $\mu_A^{\rm AUTO} = 0$.

(v) Re-assign reference galaxies to leaves of the tree generated in (i), based on the contaminated color-magnitude information.

(vi) Estimate biased mean $\hat{\beta}$ for the contaminated case as the lensing-weighted mean (i.e. with weight $w \propto \hat{\beta}$ of the leaf a galaxy falls into) of the respective $\hat{\beta}$ for each galaxy as determined in (ii) .

(vii) Estimate unbiased mean β by weighting galaxies by their biased $\hat{\beta}$ as in (vi), but using their true reference redshifts to determine the β to average.

The ratio of the two estimates in steps (vii) and (vi) (minus 1) is the $\hat{\beta}$ bias we are trying to determine. Note that at $f_{\rm ICL} = 0$, they are, by construction, identical. In other words, the decision tree is an unbiased β estimator unless the sample is affected by photometric biases or selection effects.

2.2 Model

In this section, we apply the scheme laid out in subsection 2.1 to derive an expression for the bias in $\Delta\Sigma$ as a function of ICL surface brightness, lens redshift, and depth of the source sample (Equation 2).

Judging from the surface brightness of ICL observed in Zhang (2018), the relevant range is $f_{\rm ICL} < 40$ nJy arcsec^{-2}. In this range and given the sizes and magnitudes of background galaxies,[8] ICL is a perturbation on top of the galaxies' intrinsic flux, such that we can attempt to approximate the effect of ICL on photo-z as linear. We study the linearity of biases in $\hat{\beta}$ at a range of lens redshifts $z_d = 0.2 \dots 0.8$ and limiting magnitudes of the source sample $m_{\rm lim} = 23.5 \dots 24.5$. Figure 1 shows selected results for illustration that the bias is indeed well approximated as linear in $f_{\rm ICL}$ for the most relevant regimes. Only for the highest redshift clusters are non-linear effects visible at larger ICL flux levels. This is potentially related to the fact that their background source populations are intrinsically particularly faint. In the following, we will use the measurement at $f_{\rm ICL} = 14$ nJy arcsec^{-2} (4 counts per arcsec^{-2} at ZP=30) as an anchor for the linear re-scaling. We make this choice since it allows a high signal-to-noise measurement of the slope while not suffering from systematic errors due to non-linear effects and undetected sources in CFHTLS-Deep entering the faint subsample.

For a given source depth, the slope of bias with ICL surface brightness is a function of lens redshift. By measuring the slope at a range of redshifts, we empirically find that it can be described well, within the range of $z_d = 0.2 \dots 0.8$, by a quadratic function of z_d. Measurements and quadratic model (circles and solid line) are shown in Figure 2.

In addition, we empirically find that a re-scaling of the model by $2^{m_{\rm lim}-24}$ describes the measurements reasonably well at limiting magnitudes in the range $m_{\rm lim} \in (23.5, 24.5)$ (downward and upward triangles with model as dotted and dashed curve in Figure 2). The following is the proposed model, for $g'r'i'z'$, fitted from in $z_d \in (0.2, 0.8), m_{\rm lim} \in (23.5, 24.5)$,

$$\frac{{\rm d}(\hat{\beta}/\beta)}{{\rm d}f_{\rm ICL}} \times [\mu{\rm Jy\ arcsec}^{-2}] \approx \left(2.5z_d^2 - 1.1z_d + 0.028\right) \times 2^{m_{\rm lim}-24} \ . \tag{8}$$

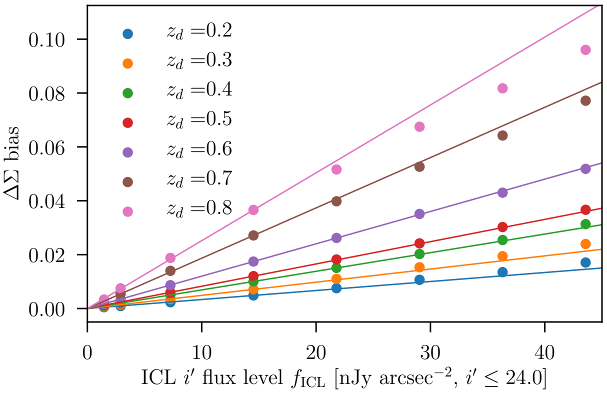

Figure 1. Bias in $\Delta\Sigma$ (defined as the negative of the bias in $\hat{\beta}$) from $g'r'i'z'$ photo-z bias for a sample of source galaxies at $20 \leq i' \leq 24$. Differently colored lines and points show results for different lens redshifts.

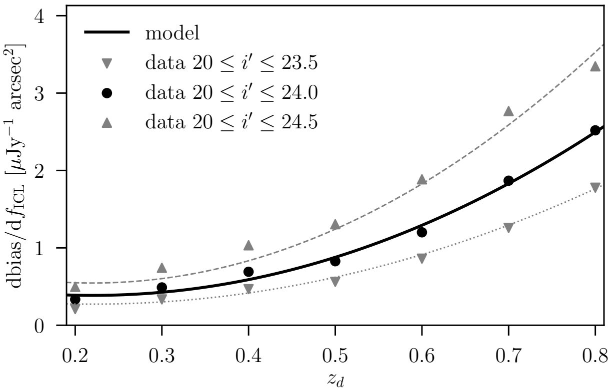

Figure 2. Slope of $\Delta\Sigma$ bias with ICL surface brightness as a function of lens redshift. Circle symbols show measurements made as in Figure 1, upward and downward triangles the same measurements, but for deeper and shallower source samples. Solid line shows a quadratic model fit to the fiducial depth, dashed and dotted lines are the same model re-scaled by 2^{m-24}, where m is the limiting magnitude of the sample.

Repeating the same analysis including $u^\star$ band gives a somewhat smaller amplitude of $(1.2z_d^2 - 0.063z_d + 0.10)$, to be rescaled the same way as a function of depth.

3 INTRA-CLUSTER LIGHT MODEL

The goal of this section is to derive a model for the surface brightness of ICL. We model it as a function of cluster mass $M_{\rm 200m}$, cluster redshift z_d, and projected physical distance r from the cluster center.

The distribution of ICL is a debated topic in the literature. It is believed that the ICL contains a significant amount of stellar mass (Behroozi et al. 2013; Contini et al. 2014; Pillepich et al. 2018), comparable to that of cluster central galaxies or the rest of the cluster galaxies. However, measurements of ICL in various samples (Zibetti et al. 2005;

---

[8] Note that an $i' = 24.5$ galaxy has a flux of 575 nJy, spread out over few arcsec^2.

Gonzalez et al. 2005; Krick et al. 2006; Toledo et al. 2011; Burke et al. 2012; Gonzalez et al. 2013; Montes & Trujillo 2014; DeMaio et al. 2015) do not necessarily find agreement on such a massive component, possibly due to methodology or conceptual differences (e.g., Morishita et al. 2017; Montes & Trujillo 2018), cluster-to-cluster variations (e.g., Krick & Bernstein 2007) or redshift evolution (e.g., Burke et al. 2015). Through averaging the light profile of ∼ 300 optically selected clusters, Zhang (2018) quantified the ICL distribution at $z \sim 0.25$ for clusters more massive than $\sim 2\times10^{14} M_\odot$. A comparison of the stellar mass in the ICL component with the total stellar mass in DES Y1 REDMAPPER clusters measured in Palmese (2018) shows that the ICL makes up ∼ 40% of the total cluster stellar mass in the sample from Zhang (2018). We make use of these measurements to model ICL.

There are three components empirically seen as diffuse light in clusters: pure ICL due to stars not bound to any galaxy, the light of faint, undetected cluster members, and scattered light of the cluster galaxies in the outskirts of the point-spread function (PSF).

We will call the first component, dominant in most regimes, *pure* ICL. This is what is measured in Zhang (2018). The PSF effect exists with every ground-based telescope at similar levels (see studies in Moffat 1969; King 1971; Racine 1996; Bernstein 2007; Sandin 2014 and also discussions in Zhang 2018). It is a contaminant to the measurement in Zhang (2018), yet greatly subdominant in the case of the DECam PSF, given that 97 per cent of light is contained within a 5" radius of the PSF (Zhang 2018, their section 4), and intrinsic ICL is a much larger fraction of total cluster light.

Our second term, the amount of light in *undetected* galaxies, depends on the depth to which cluster members are detected and can be successfully deblended. We approximate this as a fixed limiting magnitude $m^{\rm lim}$.

The full function we are trying to model is thus

$$f_{\rm ICL}(M_{200m}, z_d, r, m^{\rm lim}) = f_{\rm pure\ ICL}(M_{200m}, z_d, r) + f_{\rm undetected}(M_{200m}, z_d, r, m^{\rm lim}) \,. \tag{9}$$

We describe our model for both terms in the following sections.

3.1 Model for pure ICL

Zhang (2018) have measured the pure ICL profile around a richness-redshift selected sample of redMaPPer clusters in DES Y1 data. In this subsection, we convert their measurement of pure ICL at these fixed parameters into a prediction for $f_{\rm pure\ ICL}(M_{200m}, z_d, r)$ based on the assumptions that

- at a fixed cluster mass, ICL is due to a passively evolving stellar population. As a function of redshift, it follows the color of the red sequence, with a fixed stellar mass density profile in physical coordinates. We note that there is an ongoing debate in the literature about the growth of ICL over cosmic time, which is discussed below.
- The stellar mass density profile is self-similar, i.e. indistinguishable between different clusters when expressed as a function of r/r_{200m}. This is qualitatively consistent with the results of a richness-binned analysis in Zhang (2018).

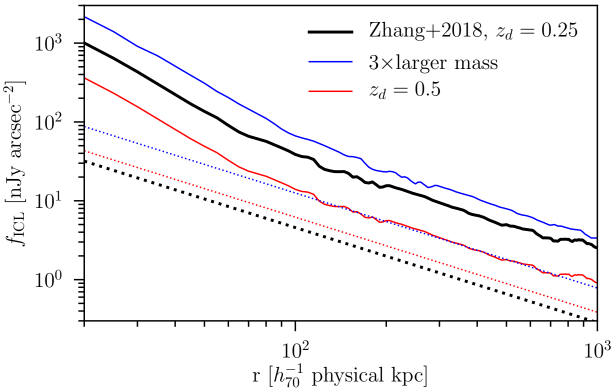

Figure 3. Pure ICL profiles (solid lines) measured in DES (black) and transformed to higher mass (blue) and redshift (red) according to Equation 10. Dotted lines show the additional ICL due to undetected cluster members (Equation 11) in a survey that detects galaxies down to $r = 22.5$.

With these assumptions, we can write

$$\begin{aligned} f^{i'}_{\rm pure\ ICL}(M_{200m}, z_d, r) &= f^{\rm Zhang}_{\rm ICL}\left(r \times \left(\frac{M_{200m}}{M^{\rm fid}_{200m}}\right)^{-1/3}\right) \\ &\times \left(\frac{D_A(z_d)}{D_A(z_{\rm fid})}\right)^2 \\ &\times 10^{-0.4\left(m_{i',z_d} - m_{\rm fid}\right)} \,, \end{aligned} \tag{10}$$

where $f^{\rm Zhang}_{\rm ICL}(r)$ is the ICL surface brightness of Zhang (2018), measured for a fiducial mass $M^{\rm fid}_{200m} = 3\times10^{14} M_\odot$ and redshift $z_{\rm fid} = 0.25$. $m_{i',z_d} - m_{\rm fid}$ is the apparent magnitude difference of a passively evolving galaxy seen at redshift z_d in CFHT i' band and at redshift $z_{\rm fid}$ in DES r' band. For the purpose of this paper, we use a Bruzual & Charlot (2003) model with solar metallicity ($Z = 0.02$), no dust, and an exponentially declining star formation history with half-time $\tau = 0.1$ and an age of 10 Gyr at $z = 0$. The ratio of angular diameters D_A corrects for the change of angular scale of the ICL profile with redshift.

Examples of ICL profiles transformed in cluster redshift, mass and filter band are shown in Figure 3. In this figure and all that follows, we apply azimuthal averaging and a smoothing of ±40kpc at $r > 150$kpc to reduce the noise of the ICL measured at large radii.

Note that we assume ICL to not accrete or eject stars over time. It is often argued that ICL forms relatively late, assembling most of its total stellar mass during galaxy interactions after redshift 1.0 (Monaco et al. 2006; Conroy et al. 2007; Burke et al. 2012; Behroozi et al. 2013; Contini et al. 2014; Zhang et al. 2016). Since our model is based on ICL measurements at $z \sim 0.25$, the luminosity of ICL at higher redshift ($z > 0.25$) is likely to be lower than, or at most equal to, the amount predicted from our passive evolution model. Hence, the photometric bias due to ICL at higher redshift ($z > 0.25$) is likely to be less severe than that predicted in the paper. Passive evolution is a conservative assumption for the purpose of estimating photo-z bias.

a [nJy arcsec^{-2}]	b_r	b_λ	b_z
9.95 ± 0.12	1.205 ± 0.010	-0.831 ± 0.037	8.96 ± 0.10

Table 1. Best–fit values for eq. (15) for the DES r' band flux from redMaPPer members. The reduced χ^2 is 1.5.

3.2 ICL from undetected cluster members

To model the contribution of undetected cluster members to diffuse light in the cluster, we use measurements of the average surface brightness due to brighter members, extrapolated with the luminosity function. The same approach is used in Zhang (2018) to remove contributions from cluster members below their threshold from the signal and arrive at a measurement of pure ICL.

We will model the light of undetected members at a given cluster-centric radius as homogeneously distributed, rather than concentrated at the positions of the actual galaxies. If the surface brightness at the positions of actual undetected galaxies is small enough so that the linearity of photo-z bias found in subsection 2.2 holds, the predicted mean bias does not depend on this assumption of homogeneity. For member galaxies with larger surface brightness that are close to the detection limit, non-linear blending effects will likely play a role - we consider these to be an issue separate to the ICL studied in this paper.

Formally, we write

$$f_{\rm undetected}(M_{200m}, z_d, r, m^{\rm lim}) = f_{\rm members}(M_{200m}, z_d, r) \times S(z_d, m^{\rm lim}, \infty)\,, \quad (11)$$

where $S(z_d, m^{\rm lim}, \infty)$ is the fraction of the integral over the cluster member luminosity function contributed by the faint end from $m^{\rm lim}$ to ∞. Note that more than 99% of the total flux as extrapolated to arbitrarily faint galaxies is contained in members brighter than $m^\star + 5$.

For a Schechter (1976) luminosity function with faint-end slope α,

$$\frac{{\rm d}N_{\rm gal}}{{\rm d}L} \propto \phi(L) \propto \left(\frac{L}{L^\star}\right)^\alpha \exp[L/L^\star]\,, \quad (12)$$

the integrated luminosity is given by

$$I(L_1, L_2) = \int_{L_1}^{L_2} L\,\phi(L)\,{\rm d}L \propto \left[\Gamma\left(\alpha+2, \frac{L_2}{L^\star}\right) - \Gamma\left(\alpha+2, \frac{L_1}{L^\star}\right)\right]\,, \quad (13)$$

with the incomplete gamma function Γ. In this work, we assume $\alpha = -1$, thus

$$S(z_d, m_1, m_2) = \Gamma\left(1, 10^{0.4(m^\star - m_1)}\right) - \Gamma\left(1, 10^{0.4(m^\star - m_2)}\right) \quad (14)$$

The characteristic magnitude $m^\star$ (Koester et al. 2007; Rykoff et al. 2014) is a function of cluster redshift z_d, which we calculate from the Bruzual & Charlot (2003) model, normalized to match the SDSS DR8 (Aihara et al. 2011) redMaPPer catalog (Rykoff et al. 2014) at $z = 0.2$.

We approximate $f_{\rm members}$ from the light of redMaPPer cluster members $f_{\rm redMaPPer}$, i.e. passive galaxies down to $0.2L_\star$. They are detected by DES over the full redshift range of the redMaPPer catalog, allowing us to empirically constrain the evolution of $f_{\rm members}$ with redshift. For $f_{\rm members}$ in Equation 11, we use the luminosity function to re-scale $f_{\rm redMaPPer}$ by a factor $I(0.2L^\star, \infty)/I(0, \infty) = 1.22$ from Equation 13, for the missing members at $L < 0.2L_\star$. In the relevant radial range, these passive galaxies dominate the cluster member population (e.g. Zu & Mandelbaum 2016).

We find that the DES r' band flux $f_{\rm members}$ of redMaPPer cluster members follows a power law in projected radial distance, cluster richness and redshift as:

$$f_{\rm members}(\lambda, z_d, r) = a\left(\frac{r}{\tilde{r}}\right)^{-b_r}\left(\frac{\lambda}{\tilde{\lambda}}\right)^{-b_\lambda}\left(\frac{1+z_d}{1+\tilde{z}_d}\right)^{-b_z}\,, \quad (15)$$

where $\tilde{r} = 240$ kpc, $\tilde{\lambda} = 40$ and $\tilde{z}_d = 0.5$ are the pivot values. Eq. (15) is fit between 20 and 1000 kpc, and the best fit results from a χ^2 minimization are given in Table 1 and r is the comoving projected distance from the cluster center in kpc. The flux used is the SExtractor `FLUX_AUTO_R` and this is weighted for each galaxy from the redMaPPer catalog by the corresponding membership probability. The masked regions are taken into account when computing the flux per area, and the errors on the flux profiles are computed through a jackknife resampling. The bins in richness ($20 < \lambda < 140$) and redshift ($0.1 < z < 0.8$) are chosen to have a similar number of clusters in most bins.

To convert $f_{\rm members}(\lambda, z_d, r)$ to $f_{\rm members}(M_{200m}, z_d, r)$ we apply the $\langle \ln\lambda | M_{500c}\rangle$ relation of Saro et al. (2015). We convert between M_{200m} and their M_{500c} using the mass-concentration relation of Duffy et al. (2008). We note that $\langle\lambda|M\rangle \neq e^{\langle \ln\lambda|M\rangle}$ due to intrinsic scatter in λ at fixed M. For the purpose of this paper and consistency with our scaling of the Zhang (2018) model for pure ICL, we set the amplitude of the scaling relation such that $\langle\lambda|M_{200m} = 3\times10^{14}M_\odot, z = 0.25\rangle$=30.

The $m_{\rm lim}$ to use with Equation 11 is dependent on survey and detection strategy. For the DES Y1 Gold catalog Drlica-Wagner et al. (2017, their Figure 8), a conservative $m_{\rm lim}$ for the purpose of estimating the contribution of cluster members to diffuse light is a DES i' band magnitude of 22.5.

We note that the contribution of undetected cluster members becomes important at large cluster mass, high redshift, and for a shallow survey (see dotted lines in Figure 3). For our DES parameters, it contributes the majority of ICL for a cluster of $M_{200m}/M_\odot = 10^{15}$ at $z_d > 0.6$. For lower mass or redshift in DES, it is a subdominant component – contributing, in the relevant regimes, between 10 and 40 per cent of ICL. For LSST it is negligible due to the completeness down to fainter magnitudes.

4 BIAS PREDICTIONS

Using the models described in section 2 and 3, we study the bias in $\Delta\Sigma$ profiles due to contamination of source photometry with diffuse light around clusters.

Due to the dependence on source population of the bias per unit ICL flux (section 2) and the dependence on cluster member detection limit of the ICL model (section 3), we need to define a limiting magnitude for the shape catalog and for the detection of cluster members in a given survey. This, in addition to the mass and redshift of a cluster sample, determines our model prediction for ICL related photo-z bias via equations (8) and (9).

We study two cases, and again choose conservative limits (i.e. faint limiting magnitudes for the shape catalog and bright limiting magnitudes for cluster member detection): (1) an ongoing *griz* wide-area survey, similar to DES, with shapes measured down to $r \approx 23.5$ (Zuntz et al. 2017) and cluster members completely detected and deblended down to $r \approx 22.5$ (Drlica-Wagner et al. 2017). And (2) an ongoing or future deep wide-area *ugriz* survey, similar to HSC or LSST, with shapes measured and cluster members completely detected and deblended down to $r \approx 25$.

Results for both cases are shown in Figure 4, for clusters of two different masses approximately spanning the range currently used for optical cluster cosmology with redMaPPer. These should be compared to the statistical uncertainties of present and future surveys (currently of the order of a few per-cent, optimistically of the order of one per-cent) for a sense of whether the biases are relevant.

We find that for a DES-like survey, even under the conservative assumptions made above, the $\Delta\Sigma$ signal estimated outside 200kpc radius is biased mostly below the one per-cent level, and only in extreme cases above the two per-cent level, even for very massive and high redshift clusters. This implies that at the scale cuts and uncertainties of present DES cluster lensing studies (McClintock et al. 2018), ICL-related photo-*z* bias is highly subdominant compared to the 5 per-cent combined statistical and systematic uncertainty.

For a significantly deeper survey like LSST, biases at the level of two per cent are possible on the small to intermediate scales of 200 – 300kpc that we hope to use for cluster lensing purposes. This is driven by the larger biases incurred by the fainter sources measured in these surveys. The availability of *u* band information in addition to *griz* somewhat alleviates the effect. Given the conservative assumptions made in our study, it is conceivable that the actual bias is only a fraction from our model prediction. But at least for the massive end of the clusters studied with these surveys, diffuse light photo-*z* contamination requires either more detailed investigation or more conservative cuts in radius or limiting source magnitude.

4.1 Limitations of our model

In the context of these predictions, we summarize the simplifications made in our model, and their likely effect on the bias in practical applications.

Simplifications, i.e. assumptions we had to make due to limited understanding of physical or algorithmic details:

- **generic photo-*z* algorithm:** For the purpose of this test, we used a simple empirical photo-*z* algorithm. Assuming that all photo-*z* algorithms estimate the same relation of multi-band flux and redshift, results for other algorithms would likely be similar, yet not equal. We have made simplified tests using BPZ (Benítez 2000; Hoyle et al. 2017) that indicate that this is indeed the case.
- **leakage of ICL into galaxy photometry:** We assumed leakage to be proportional to a circular aperture with the post-seeing half-light radius of the galaxy. This is an approximation of how a matched aperture or, equivalently, model fitting algorithm for photometric measurements might perform. While we match the leakage scale in this work to the mean observed change in SExtractor `DETMODEL` flux, other photometry measurement algorithms might show very different results, and galaxy morphology might affect the leakage scale in a galaxy type and redshift dependent way. Also, small scale background subtraction could greatly reduce (or even invert) the effect. It is advisable that the leakage of diffuse light into galaxy photometry is estimated from image simulations for any lensing analysis that aims at a per-cent level accuracy.
- **linearity of β bias as a function of ICL flux:** Our model assumes that the change in estimated lensing amplitude $\hat{\beta}$ is linear in the ICL surface brightness. While this is appropriate for the relevant range of mean ICL surface brightness, inhomogeneity (i.e. due to undetected yet localized cluster members) could affect the photo-*z* more or less than predicted here. At the level of deblending possible with present and future lensing surveys, we expect this effect to be subdominant.
- **pure red cluster member population:** We have assumed that the cluster galaxy population only contains passive galaxies, similar in color to the ones identified by the redMaPPer algorithm. In practice, clusters contain star forming galaxies, especially at lower mass and higher redshift. The light of the undetected members among them is likely to have a similar, but not quite equal, effect on photo-*z* bias as the light of red members. On the radial scales considered here, star-forming members are, however, not a majority of the population. In addition, the light of undetected cluster members is a subdominant component relative to pure ICL, hence we do not expect this assumption to significantly change our conclusions.
- **self-similar scaling of pure ICL:** We have assumed that pure ICL scales self-similarly with cluster mass, i.e. its surface brightness is fixed at a given projected r/r_{500}. While this is consistent with simple comparisons made in Zhang (2018), a more detailed study could reveal deviations.

Conservative assumptions, i.e. ways in which we likely overestimate the effect of ICL in practice:

- **passive SED of ICL:** We assume ICL to share the color of passive galaxies at the cluster redshift. A population of younger stars in the ICL would likely reduce its effect on photo-*z* bias due to its similarity in color to background galaxies.
- **conservative deblending limits:** For DES, we have assumed cluster members to be deblended and thus not affecting source photo-*z* down to a magnitude limit of $r = 22.5$. At this level, DES Y1 is highly complete – a significant fraction of cluster members below this limit are likely deblended successfully and, unlike assumed, do not in fact contribute to diffuse ICL. As a result, we likely overestimate the associated photo-*z* bias in DES, in particular at large cluster mass and redshift.
- **magnitude limited source sample:** We used a simple magnitude cut to define our source sample. Realistic lensing source samples have additional selection criteria. A choice of limiting magnitude at the faint end of the population that is used in a given analysis allows for a conservative prediction of potential biases. For DES Y1/Y3 data, this was possible to do in this work.

Limitations, i.e. regimes in which our model is not reliable:

- **faint limit of source sample:** For LSST, sufficiently faint reference samples of galaxies with known redshift and

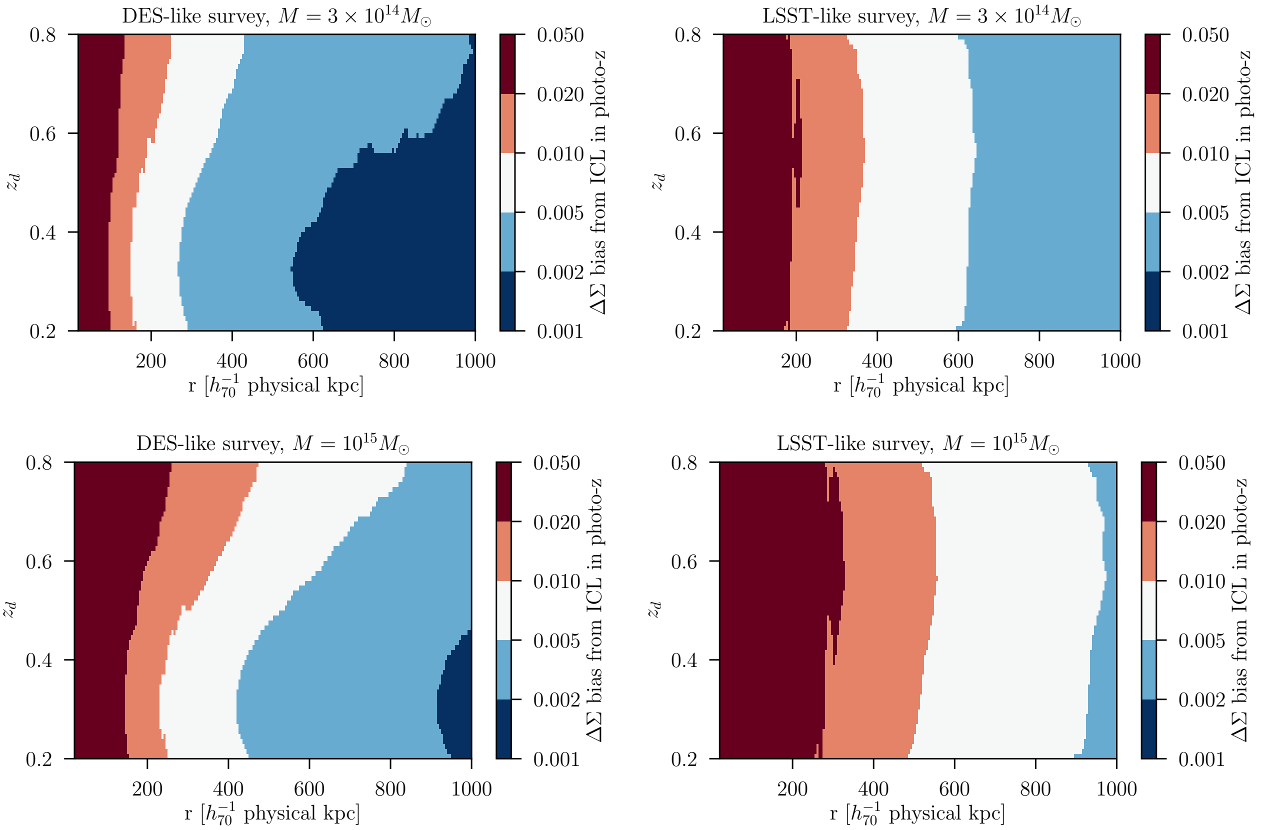

Figure 4. Predictions for the bias in $\Delta\Sigma$ profiles due to ICL-related source photo-z bias for a DES-like (left-hand panels) and LSST-like (right-hand panels) survey, and a cluster of $M_{200m}/M_\odot = 3 \times 10^{14}$ (top) and 10^{15} (bottom). The smallest scales (e.g. $r < 200 h_{70}^{-1}$ kpc in McClintock et al. 2018) that are most heavily affected by ICL are commonly excised from cluster lensing analyses for other reasons.

flux measurements do not exist to extend the modeling beyond $i' \approx 25$. Assuming that fainter lensing samples are used, the bias derived here is an underestimate of the bias encountered by such analyses.

- **blending with cluster members:** We only attempt to model diffuse ICL leaking into source photometry at a subdominant level. For the effect of blending between similarly bright cluster member and background galaxies, the model developed here is not applicable. Besides, the success of correctly treating these cases will likely strongly depend on the choice of deblending algorithm.

5 CONCLUSIONS

We have developed a model for the bias in weak lensing estimates of cluster surface mass overdensity due to the contamination of lensed galaxy photometry from diffuse intracluster light. The latter systematically changes the flux, color, and thus photometric redshift estimate of the faint galaxies used as lensing sources.

Our model for diffuse light in clusters is simplistic yet conservative for the purpose of this exercise: a pure component of ICL due to un-bound stars in the cluster potential, measured at low redshift (Zhang 2018) and re-scaled in mass and redshift by assuming self-similarity and passive evolution; and a component due to stars in undetected, faint cluster members, extrapolated from detected galaxies by means of the luminosity function. The effect of this surface brightness on photo-z is estimated from an idealized empirical photo-z estimation scheme (Gruen & Brimioulle 2016).

We find that for a DES-like cluster lensing experiment, i.e. with cluster masses up to $M_{200m} = 10^{15} M_\odot$, detection and deblending of cluster members brighter than $i' = 22.5$, and a source sample no fainter than $i' = 23.5$, ICL-related photo-z bias does not significantly affect weak lensing mass reconstruction. Outside a cluster-centric radius of 200kpc, which is commonly excluded in lensing studies for other reasons, biases are typically below 1 per cent for an M_{200m} $3 \times 10^{14} M_\odot$ cluster, and below 2 per cent at M_{200m} $10^{15} M_\odot$, even under the conservative assumptions we make. The effect of ICL on measured galaxy shapes may well be larger than that, and should be tested with dedicated image simulations.

Deeper source catalogs will be somewhat more susceptible to ICL-related photo-z biases because the flux and color of faint source galaxies can be changed more strongly by ICL contamination. For massive clusters, shape catalogs down to $i' = 25$ show one per-cent biases at approximately twice the radius as the above DES-like survey. Even fainter sources will likely show even stronger effects, although this is difficult to quantify at present due to the lack of reliable color-magnitude-redshift information for such samples. An explicit treatment of measured fluxes as a composite of intra-cluster and background galaxy light in photo-z estimation could in principle remedy this effect. With moderately conservative scale and magnitude cuts, however, ICL bias of photo-z will be a non-issue even in the next generation of surveys – and with a less conservative examination of the effect, these could likely be moderately relaxed from the recommendations given in this work.

ACKNOWLEDGEMENTS

Support for DG was provided by NASA through the Einstein Fellowship Program, grant PF5-160138.

The authors thank Fabrice Brimioulle for providing the CFHTLS Deep photometry and photo-z catalogs used in this work. This work has been promoted by fruitful discussions during the workshop series "Becoming a One-Percenter".

Funding for the DES Projects has been provided by the U.S. Department of Energy, the U.S. National Science Foundation, the Ministry of Science and Education of Spain, the Science and Technology Facilities Council of the United Kingdom, the Higher Education Funding Council for England, the National Center for Supercomputing Applications at the University of Illinois at Urbana-Champaign, the Kavli Institute of Cosmological Physics at the University of Chicago, the Center for Cosmology and Astro-Particle Physics at the Ohio State University, the Mitchell Institute for Fundamental Physics and Astronomy at Texas A&M University, Financiadora de Estudos e Projetos, Fundação Carlos Chagas Filho de Amparo à Pesquisa do Estado do Rio de Janeiro, Conselho Nacional de Desenvolvimento Científico e Tecnológico and the Ministério da Ciência, Tecnologia e Inovação, the Deutsche Forschungsgemeinschaft and the Collaborating Institutions in the Dark Energy Survey.

The Collaborating Institutions are Argonne National Laboratory, the University of California at Santa Cruz, the University of Cambridge, Centro de Investigaciones Energéticas, Medioambientales y Tecnológicas-Madrid, the University of Chicago, University College London, the DES-Brazil Consortium, the University of Edinburgh, the Eidgenössische Technische Hochschule (ETH) Zürich, Fermi National Accelerator Laboratory, the University of Illinois at Urbana-Champaign, the Institut de Ciències de l'Espai (IEEC/CSIC), the Institut de Física d'Altes Energies, Lawrence Berkeley National Laboratory, the Ludwig-Maximilians Universität München and the associated Excellence Cluster Universe, the University of Michigan, the National Optical Astronomy Observatory, the University of Nottingham, The Ohio State University, the University of Pennsylvania, the University of Portsmouth, SLAC National Accelerator Laboratory, Stanford University, the University of Sussex, Texas A&M University, and the OzDES Membership Consortium.

Based in part on observations at Cerro Tololo Inter-American Observatory, National Optical Astronomy Observatory, which is operated by the Association of Universities for Research in Astronomy (AURA) under a cooperative agreement with the National Science Foundation.

The DES data management system is supported by the National Science Foundation under Grant Numbers AST-1138766 and AST-1536171. The DES participants from Spanish institutions are partially supported by MINECO under grants AYA2015-71825, ESP2015-66861, FPA2015-68048, SEV-2016-0588, SEV-2016-0597, and MDM-2015-0509, some of which include ERDF funds from the European Union. IFAE is partially funded by the CERCA program of the Generalitat de Catalunya. Research leading to these results has received funding from the European Research Council under the European Union's Seventh Framework Program (FP7/2007-2013) including ERC grant agreements 240672, 291329, and 306478. We acknowledge support from the Australian Research Council Centre of Excellence for All-sky Astrophysics (CAASTRO), through project number CE110001020, and the Brazilian Instituto Nacional de Ciência e Tecnologia (INCT) e-Universe (CNPq grant 465376/2014-2).

This manuscript has been authored by Fermi Research Alliance, LLC under Contract No. DE-AC02-07CH11359 with the U.S. Department of Energy, Office of Science, Office of High Energy Physics. The United States Government retains and the publisher, by accepting the article for publication, acknowledges that the United States Government retains a non-exclusive, paid-up, irrevocable, world-wide license to publish or reproduce the published form of this manuscript, or allow others to do so, for United States Government purposes.

Based in part on observations obtained with MegaPrime/MegaCam, a joint project of CFHT and CEA/IRFU, at the Canada-France-Hawaii Telescope (CFHT) which is operated by the National Research Council (NRC) of Canada, the Institut National des Science de l'Univers of the Centre National de la Recherche Scientifique (CNRS) of France, and the University of Hawaii. This work is based in part on data products produced at Terapix available at the Canadian Astronomy Data Centre as part of the Canada-France-Hawaii Telescope Legacy Survey, a collaborative project of NRC and CNRS.

This paper has gone through internal review by the DES collaboration.

REFERENCES

Aihara H., et al., 2011, ApJS, 193, 29

Bartelmann M., Schneider P., 2001, Phys. Rep., 340, 291

Becker M. R., Kravtsov A. V., 2011, ApJ, 740, 25

Behroozi P. S., Wechsler R. H., Conroy C., 2013, ApJ, 770, 57

Benítez N., 2000, ApJ, 536, 571

Bernstein R. A., 2007, ApJ, 666, 663

Bruzual G., Charlot S., 2003, Mon. Not. Roy. Astron. Soc., 344, 1000

Burke C., Collins C. A., Stott J. P., Hilton M., 2012, MNRAS, 425, 2058

Burke C., Hilton M., Collins C., 2015, MNRAS, 449, 2353

Chang C., et al., 2017, preprint, (`arXiv:1710.06808`)

Conroy C., Wechsler R. H., Kravtsov A. V., 2007, ApJ, 668, 826

Contini E., De Lucia G., Villalobos Á., Borgani S., 2014, MNRAS, 437, 3787

DeMaio T., Gonzalez A. H., Zabludoff A., Zaritsky D., Bradač M., 2015, MNRAS, 448, 1162

DeMaio T., Gonzalez A. H., Zabludoff A., Zaritsky D., Connor T., Donahue M., Mulchaey J. S., 2018, MNRAS, 474, 3009

Dietrich J. P., et al., 2017a, preprint, (`arXiv:1711.05344`)

Dietrich J. P., et al., 2017b, preprint, (`arXiv:1711.05344`)

Drlica-Wagner A., et al., 2017, preprint, (`arXiv:1708.01531`)

Duffy A. R., Schaye J., Kay S. T., Dalla Vecchia C., 2008, Mon. Not. Roy. Astron. Soc., 390, L64
Gonzalez A. H., Zabludoff A. I., Zaritsky D., 2005, ApJ, 618, 195
Gonzalez A. H., Sivanandam S., Zabludoff A. I., Zaritsky D., 2013, ApJ, 778, 14
Gruen D., Brimioulle F., 2016, preprint, (`arXiv:1610.01160`)
Gruen D., et al., 2014, MNRAS, 442, 1507
Hoekstra H., Herbonnet R., Muzzin A., Babul A., Mahdavi A., Viola M., Cacciato M., 2015, preprint, p. 1502.01883 (`arXiv:1502.01883`)
Hoyle B., et al., 2017, preprint, (`arXiv:1708.01532`)
King I. R., 1971, PASP, 83, 199
Koester B. P., et al., 2007, ApJ, 660, 221
Kravtsov A. V., Vikhlinin A. A., Meshcheryakov A. V., 2018, Astronomy Letters, 44, 8
Krick J. E., Bernstein R. A., 2007, AJ, 134, 466
Krick J. E., Bernstein R. A., Pimbblet K. A., 2006, AJ, 131, 168
McClintock T., et al., 2018, preprint, (`arXiv:1805.00039`)
Medezinski E., et al., 2017, preprint, (`arXiv:1706.00427`)
Melchior P., et al., 2017, Mon. Not. Roy. Astron. Soc., 469, 4899
Mihos C., 2015, IAU General Assembly, 22, 2247903
Moffat A. F. J., 1969, A&A, 3, 455
Monaco P., Murante G., Borgani S., Fontanot F., 2006, ApJ, 652, L89
Montes M., Trujillo I., 2014, ApJ, 794, 137
Montes M., Trujillo I., 2018, MNRAS, 474, 917
Morishita T., Abramson L. E., Treu T., Schmidt K. B., Vulcani B., Wang X., 2017, ApJ, 846, 139
Okabe N., Smith G. P., 2016, Mon. Not. Roy. Astron. Soc., 461, 3794
Palmese A. e. a., 2018
Pillepich A., et al., 2018, MNRAS, 475, 648
Racine R., 1996, PASP, 108, 699
Rykoff E. S., et al., 2014, ApJ, 785, 104
Sandin C., 2014, A&A, 567, A97
Saro A., et al., 2015, Mon. Not. Roy. Astron. Soc., 454, 2305
Schechter P., 1976, ApJ, 203, 297
Sheldon E. S., et al., 2004, AJ, 127, 2544
Simet M., McClintock T., Mandelbaum R., Rozo E., Rykoff E., Sheldon E., Wechsler R. H., 2017, Mon. Not. Roy. Astron. Soc., 466, 3103
Stern C., et al., 2018, preprint, (`arXiv:1802.04533`)
Toledo I., Melnick J., Selman F., Quintana H., Giraud E., Zelaya P., 2011, MNRAS, 414, 602
Varga et al. 2018, "in preparation"
Zhang Y. e. a., 2018
Zhang Y., et al., 2016, ApJ, 816, 98
Zibetti S., White S. D. M., Schneider D. P., Brinkmann J., 2005, MNRAS, 358, 949
Zu Y., Mandelbaum R., 2016, MNRAS, 457, 4360
Zuntz J., et al., 2017, preprint, (`arXiv:1708.01533`)
Zwicky F., 1951, PASP, 63, 61
Zwicky F., 1952, PASP, 64, 242
von der Linden A., et al., 2014, MNRAS, 443, 1973

APPENDIX A: EFFECT OF ICL ON BOOST FACTOR ESTIMATES

Leakage of cluster members into the background source sample is a well-known cause for systematic error in cluster lensing. Because cluster members are not gravitationally lensed, but the redshifts of those that make it into the background source sample overestimated, this reduces the amplitude of the measured shear signal relative to a model prediction based on the estimated redshifts. Many analyses, especially those suffering from relatively poor photometric information that does not allow a pure background selection without great losses in sample size, have used a radially dependent *boost factor* correction (Sheldon et al. 2004). That is, they divided the measured signal (or multiplied the model prediction) by a factor equal to the fraction of lensing weight actually due to non-member galaxies (e.g. Melchior et al. 2017; McClintock et al. 2018).

The quantity needed for this correction is the fraction of lensing weight due to cluster members $f_{\rm cl}$ in each radial bin. This has often been estimated from the clustering of background sources with the lens positions. The blending of sources with large, bright cluster member galaxies is a known contaminant that is, however, difficult to quantify and correct.

A different way of finding $f_{\rm cl}$ is based on the decomposition of the estimated, lensing weighted $p_{\rm est}(z)$ into a component measured in non-cluster fields $p_{\rm field}(z)$ and a component with different shape due to contaminating cluster members $p_{\rm member}(z)$, as

$$p_{\rm est}(z) = (1 - f_{\rm cl}) \times p_{\rm field}(z) + f_{\rm cl} \times p_{\rm member}(z) \; . \qquad \text{(A1)}$$

This method, developed in a series of papers (Gruen et al. 2014; Melchior et al. 2017; Varga et al. 2018) and applied in several other works (Medezinski et al. 2017; Dietrich et al. 2017b; Chang et al. 2017; Stern et al. 2018) has the advantage that it is at first order insensitive to blending. It is, however, potentially susceptible to photo-z biases and source redshift dependent selection effects in the vicinity of the cluster (see also the note in Medezinski et al. 2017, their section 6.2).

We test the effect of ICL leakage into photometry on boost factors estimated with Equation A1. Specifically, we use the scheme implemented in Melchior et al. (2017) and McClintock et al. (2018) and validated in Varga et al. (2018) to check the methodology of these studies in the presence of ICL. Here, $p_{\rm member}$ is assumed to be a Gaussian distribution. Its mean and width are varied, alongside $f_{\rm cl}$, to find the best-fitting boost factor in a least-squared metric between the left and right side of Equation A1.

We simulate the presence of a member population of a cluster at redshift z_d by mixing the redshift distribution of a magnitude limited sample of $i' < 23.5$ with a Gaussian of mean $z_d + 0.1$ and width $\sigma_z = 0.1$.

For true contaminations $f_{\rm cl} = 0.1, 0.2, 0.4$ and lens redshifts between $z_d \in [0.2, 0.6]$, common for the settings in (Melchior et al. 2017; McClintock et al. 2018), the maximum bias introduced by ICL in our model at $f_{\rm ICL} = 15$nJ arcsec^{-2} is $\Delta f_{\rm cl} = 0.008$, or

$$\frac{{\rm d}f_{\rm cl}}{{\rm d}f_{\rm ICL}} \lesssim 0.0005 \; . \qquad \text{(A2)}$$

This is to be interpreted as a multiplicative bias on $\Delta\Sigma$ and significantly smaller than the effect on β shown in Figure 1. Where the latter is negligible, ICL does therefore not significantly impact boost factors estimated from $p(z)$ decomposition.

AFFILIATIONS

[1] Kavli Institute for Particle Astrophysics & Cosmology, P. O. Box 2450, Stanford University, Stanford, CA 94305, USA
[2] SLAC National Accelerator Laboratory, Menlo Park, CA 94025, USA
[3] Fermi National Accelerator Laboratory, P. O. Box 500, Batavia, IL 60510, USA
[4] Department of Physics & Astronomy, University College London, Gower Street, London, WC1E 6BT, UK
[5] Departamento de Física Matemática, Instituto de Física, Universidade de São Paulo, CP 66318, São Paulo, SP, 05314-970, Brazil
[6] Laboratório Interinstitucional de e-Astronomia - LIneA, Rua Gal. José Cristino 77, Rio de Janeiro, RJ - 20921-400, Brazil
[7] Max Planck Institute for Extraterrestrial Physics, Giessenbachstrasse, 85748 Garching, Germany
[8] Universitäts-Sternwarte, Fakultät für Physik, Ludwig-Maximilians Universität München, Scheinerstr. 1, 81679 München, Germany
[9] Department of Astrophysical Sciences, Princeton University, Peyton Hall, Princeton, NJ 08544, USA
[10] Department of Astronomy, University of Michigan, Ann Arbor, MI 48109, USA
[11] Department of Physics, University of Michigan, Ann Arbor, MI 48109, USA
[12] Department of Physics, University of Arizona, Tucson, AZ 85721, USA
[13] Department of Physics and Electronics, Rhodes University, PO Box 94, Grahamstown, 6140, South Africa
[14] Institute of Cosmology & Gravitation, University of Portsmouth, Portsmouth, PO1 3FX, UK
[15] Observatório Nacional, Rua Gal. José Cristino 77, Rio de Janeiro, RJ - 20921-400, Brazil
[16] Department of Astronomy, University of Illinois at Urbana-Champaign, 1002 W. Green Street, Urbana, IL 61801, USA
[17] National Center for Supercomputing Applications, 1205 West Clark St., Urbana, IL 61801, USA
[18] Institut de Física d'Altes Energies (IFAE), The Barcelona Institute of Science and Technology, Campus UAB, 08193 Bellaterra (Barcelona) Spain
[19] Kavli Institute for Cosmological Physics, University of Chicago, Chicago, IL 60637, USA
[20] Institut d'Estudis Espacials de Catalunya (IEEC), 08193 Barcelona, Spain
[21] Institute of Space Sciences (ICE, CSIC), Campus UAB, Carrer de Can Magrans, s/n, 08193 Barcelona, Spain
[22] Centro de Investigaciones Energéticas, Medioambientales y Tecnológicas (CIEMAT), Madrid, Spain
[23] Department of Physics, IIT Hyderabad, Kandi, Telangana 502285, India
[24] Excellence Cluster Universe, Boltzmannstr. 2, 85748 Garching, Germany
[25] Faculty of Physics, Ludwig-Maximilians-Universität, Scheinerstr. 1, 81679 Munich, Germany
[26] Instituto de Fisica Teorica UAM/CSIC, Universidad Autonoma de Madrid, 28049 Madrid, Spain
[27] Santa Cruz Institute for Particle Physics, Santa Cruz, CA 95064, USA
[28] Center for Cosmology and Astro-Particle Physics, The Ohio State University, Columbus, OH 43210, USA
[29] Department of Physics, The Ohio State University, Columbus, OH 43210, USA
[30] Harvard-Smithsonian Center for Astrophysics, Cambridge, MA 02138, USA
[31] Department of Astronomy/Steward Observatory, 933 North Cherry Avenue, Tucson, AZ 85721-0065, USA
[32] Australian Astronomical Observatory, North Ryde, NSW 2113, Australia
[33] George P. and Cynthia Woods Mitchell Institute for Fundamental Physics and Astronomy, and Department of Physics and Astronomy, Texas A&M University, College Station, TX 77843, USA
[34] Institució Catalana de Recerca i Estudis Avançats, E-08010 Barcelona, Spain
[35] Jet Propulsion Laboratory, California Institute of Technology, 4800 Oak Grove Dr., Pasadena, CA 91109, USA
[36] Department of Physics and Astronomy, Pevensey Building, University of Sussex, Brighton, BN1 9QH, UK
[37] School of Physics and Astronomy, University of Southampton, Southampton, SO17 1BJ, UK
[38] Brandeis University, Physics Department, 415 South Street, Waltham MA 02453
[39] Instituto de Física Gleb Wataghin, Universidade Estadual de Campinas, 13083-859, Campinas, SP, Brazil
[40] Computer Science and Mathematics Division, Oak Ridge National Laboratory, Oak Ridge, TN 37831
[41] Argonne National Laboratory, 9700 South Cass Avenue, Lemont, IL 60439, USA
[42] Cerro Tololo Inter-American Observatory, National Optical Astronomy Observatory, Casilla 603, La Serena, Chile

This paper has been typeset from a TEX/LATEX file prepared by the author.